Pendulum-like Oscillation Controller for UAV Based on Lévy-flight Pigeon-inspired Optimization and LQR

Zhuqing Liu, Haibin Duan, *Senior Member, IEEE*, Yijun Yang, Xiaoguang Hu
School of Automation Science and Electrical Engineering
Beihang University (BUAA), Beijing, 100083, China
Email: zhuqingliu@buaa.edu.cn; hbduan@buaa.edu.cn

***Abstract*—A new method for parameter optimization of pendulum-like oscillation controller in uninhabited aerial vehicles (UAVs) is presented, which is named Lévy -flight pigeon-inspired optimization (LFPIO) algorithm. The algorithm is based on Linear-quadratic Regulator (LQR), which help the controller with greater precision and better performance on feasibility, effectiveness and robustness. As a consequence, LFPIO can find the optimal value accurately and circumvent the premature convergence problems. Experimental results and conclusion are given by the performance of this new algorithm and compared with basic pigeon-inspired optimization (PIO), particle swarm optimization (PSO), particle swarm optimization and simulated annealing (SAPSO). The comparative results verify the effectiveness of LFPIO.**

Keywords—uninhabited aerial vehicles (UAVs), Lévy -flight, pigeon-inspired optimization (PIO), pendulum-like oscillation, linear-quadratic regulator (LQR).

I. INTRODUCTION

Uninhabited aerial vehicles (UAVs) can offer many advantages for its low cost, small volume, low weight and flexible flight. UAV can adapt to complicated environment where human cannot approach in the emergency situation to which could help reduce the risk of the human participation which led them well suitable to many kinds of missions [1]. The UAV with duct fun has higher aerodynamic efficiency higher safety and smaller size compared with other unmanned helicopters. These features make them well suited for both military as well as civil fields[2].

Great contributions has been made in UAV's development [3]. In recent years, navigation approaches, control law designs and aerodynamics analysis of UAVs were out forward. A new approach to position and orientation estimation for vision-based UAV navigation is proposed [4]. A new method for controller design Swarm intelligence and artificial brain is provided[5]. Several bio-inspired computation algorithms used in UAV's controller is applied [6][7]. Dynamics of UAV which allows an efficient stabilization of the normally unstable model by using a nonlinear closed-loop control law has been designed [8].

UAV has the ability to hover and stare, and the flexibility in all directions. They are designed to perform reconnaissance missions and surveillance [9]. The external disturbances and other uncertainties of the constraints had bad effect on the pendulum-like oscillation, resulting in vagued images, even UAVs' overturning [9].As we can see, the control techniques for UAVs about the hover and stare state has great significant in reconnaissance missions and surveillance[11].

PSO algorithm is a bio-inspired computation techniques. It can solve complex optimization problems.[12]. Particle swarm optimization and simulated annealing (SAPSO) is an improved-PSO algorithm proposed in 2012 [13]. The algorithm can evade shortcomings which the standard PSO has. In spite of that, SAPSO will become undependable in solving complicated function. PIO is a population-based swarm intelligence artificial algorithm which imitates the behavior of pigeons proposed by Duan in 2014 [14]. PIO is an effective algorithm, but it still have some problems in feasibility and effectiveness. To resolve these problems, a new swarm intelligence is used in this paper.

In this paper, Lévy-flight pigeon-inspired optimization (LFPIO) algorithm for parameter optimization of matrixed Q and R in the linear-quadratic regulator is proposed which is based on linear-quadratic regulator (LQR). This way make great effort for the UAV's dynamic properties efficiently while implementing reconnaissance missions.

The rest of the paper is presented as follows: The mathematical model of the UAV pendulum-like oscillation is first introduced in the following section. Then, a hybrid LQR controller based on LFPIO is developed in Section 3. Finally, a series of experiments are presented in Section4 and our concluding remarks are contained in Section 5.

II .MATHEMATICAL MODEL OF UAV PENDULUM-LIKE OSCILLATION

In this paper, the UAV uses the axial symmetrical layout [15]. In this section, the Lagrangian method is using for the pendulum-like oscillation, and the neighborhood of the hover and stare equilibrium is obtained by the corresponding linearized model.

The system of nonlinear mathematical model of UAV pendulum-like oscillation consists the suspension point O_1, the starting point O_1 which can be seen in the figure 1. The ground-fixed coordinate system OXYZ with a pendulum rod O_1O_2 and the pendulum mass O_2 (see Fig.1). It parallel to a flexible ground coordinate system OXYZ. $O_1x_2y_2z_2$ originates from O_1 and axis z_2 points downward along the pendulum rod O_1O_2 which is the subject of pendulum model coordinate system. 2-dimesion pendulum-like oscillation have decomposed to one in the direction of axis X and Y. The transition Matrix R from O_1

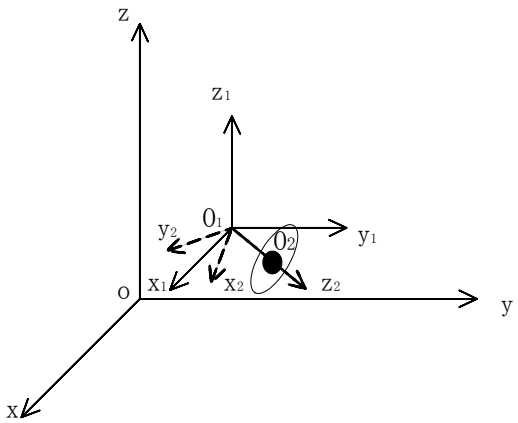

(1) Pendulum model's coordinates

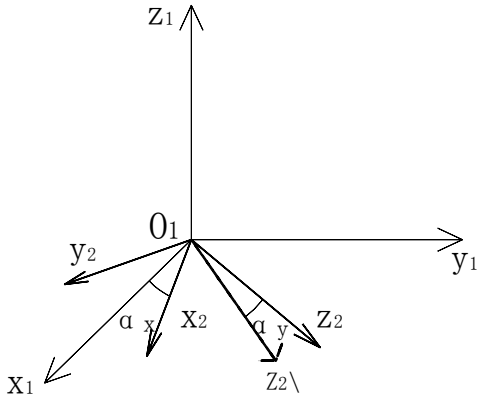

(2) Decomposition of oscillation angle

Fig.1 Pendulum model's coordinates and decomposition of oscillation angle

$x_2\ y_2\ z_2$ to $O_2\ x_1\ y_1\ z_1$ is obtained as follows:

$$R=\begin{bmatrix} cos\alpha_y & sin\alpha_x sin\alpha_y & cos\alpha_x sin\alpha_y \\ 0 & cos\alpha_x & -sin\alpha_x \\ -sin\alpha_y & sin\alpha_x cos\alpha_y & cos\alpha_x cos\alpha_y \end{bmatrix} \quad (1)$$

Suppose the position vector of the pendulum mass O_2 in the coordinate frame of $O_1\ x_2\ y_2\ z_2$ and the suspension point O_1 in $OXYZ$ are presented with, $r_2'=[0,0,l]^T$, $r_1=[x,y,z]^T$ respectively. Then, the coordinate of point O_2 in the coordinate frame of $O_1\ x_1\ y_1\ z_1$ can be calculated as follows:

$$r_{12}=R\cdot r_2'=[l\cos\alpha_x\sin\alpha_y,-l\sin\alpha_x,l\cos\alpha_x\cos\alpha_y]^T \quad (2)$$

l represents the length of the pendulum which is from O_2 to O_1 .

Coordinate of O_2 presented as follows:

$$r_2=r_1+R\cdot r_2' \quad (3)$$

Pendulum system by using the Lagrange function is as follows:

$$L=T_0-V=T_m+T_M'+T_M''-V$$

$$=\frac{1}{2}mr_h^{\dot{T}}r_{\dot{h}}+\frac{1}{2}m_t V_t^T V+\frac{1}{2}J_{x2}\omega_{x2}^2+\frac{1}{2}J_{y2}\omega_{y2}^2$$

$$-(-m_t gl\cos\alpha_x\cos\alpha_y+(m+m_t)(z-z_0))$$

$$=\frac{1}{2}(m+m_t)(\dot{x}^2+\dot{y}^2+\dot{z}^2)$$

$$+\frac{1}{6}m_t l[(3+cos^2\alpha_y)l\dot{\alpha}_x^{\,2}+(1+3cos^2\alpha_x)l\dot{\alpha}_y^{\,2}$$

$$+m_t l(\dot{x}\dot{\alpha}_y\cos\alpha_x\cos\alpha_y-\dot{x}\dot{\alpha}_x\sin\alpha_x\sin\alpha_y-\dot{y}\dot{\alpha}_x\cos\alpha_x$$

$$-\dot{z}\dot{\alpha}_x\sin\alpha_x\cos\alpha_y-\dot{z}\dot{\alpha}_y\cos\alpha_x\sin\alpha_y+m_t gl\cos\alpha_x\cos\alpha_y$$

$$-(m+m_t)(z-z_0)g \quad (4)$$

The potential energy of the system is shown as V. The zero-potential energy surface is selected at the commence state of the pendulum-like oscillation. In addition, T_M', T_M, T_M'' represents respectively translation kinetic energy of the pendulum mass O_2, kinetic energy of the suspension center O_1, rotational kinetic energy of the pendulum rod around the centroid of O_2

Thus, formula (5) can be deduced from the Lagrange equation as follows:

$$\begin{cases} \frac{d}{dt}\left(\frac{\partial L}{\partial\dot{\alpha}_x}\right)-\frac{\partial L}{\partial\alpha_x}=0 \\ \frac{d}{dt}\left(\frac{\partial L}{\partial\dot{\alpha}_y}\right)-\frac{\partial L}{\partial\alpha_y}=0 \end{cases} \quad (5)$$

The non-linear mathematical model of the UAV pendulum-like oscillation is presented as follows.

$$\begin{cases} \ddot{\alpha}_x=(3\ddot{x}sin\alpha_x sin\alpha_y+3\ddot{y}cos\alpha_x+3\ddot{z}sin\alpha_x cos\alpha_y \\ \quad +2d\dot{\alpha}_x\dot{\alpha}_y cos\alpha_x sin\alpha_y-3d\dot{\alpha}_y^{\,2}sin\alpha_x cos\alpha_y \\ \quad -3gsin\alpha_x cos\alpha_x)/(cos^2\alpha_y+3)d \\ \ddot{\alpha}_y=(-3\ddot{x}cos\alpha_x cos\alpha_y+3\ddot{z}cos\alpha_x sin\alpha_y \\ \quad +6d\dot{\alpha}_x\dot{\alpha}_y sin\alpha_x cos\alpha_x-d\dot{\alpha}_x^{\,2}sin\alpha_y cos\alpha_y \\ \quad -3gcos\alpha_x sin\alpha_x)/(cos^2\alpha_x+3)d \end{cases} \quad (6)$$

Change the pendulum angle around axis x, y (α_x, α_y) to the pitch and roll angle β_x,β_y according to$\beta_x=\alpha_y$, $\beta_y=-\alpha_x$, and then formula (6) can be described as:

$$\begin{cases} \ddot{\beta}_x=(3\ddot{x}sin\beta_x sin\beta_y+3\ddot{y}cos\beta_x+3\ddot{z}sin\beta_x cos\beta_y \\ \quad +2d\dot{\beta}_x\dot{\beta}_y cos\beta_x sin\beta_y-3d\dot{\alpha}_y{}^2 sin\beta_x cos\beta_y \\ \quad -3gsin\beta_x cos\beta_x)/(cos^2\alpha_y+3)d \\ \ddot{\alpha}_y=(-3\ddot{x}cos\beta_x cos\beta_y+3\ddot{z}cos\beta_x sin\beta_y \\ \quad +6d\dot{\beta}_x\dot{\beta}_y sin\beta_x cos\beta_x-d\dot{\beta}_x{}^2 sin\beta_y cos\beta_y \\ \quad -3gcos\beta_x sin\beta_x)/(cos^2\beta_x+3)d \end{cases} \tag{7}$$

Choose the state variables $X_e=[x,\partial_x,\dot{x},y,\partial_y,\dot{y},z,\dot{z},\ddot{x},\ddot{y},\ddot{z}]^T$, the input of the system $u=[\ddot{x},\ddot{y}]^T$.

The results on the linear model of the pendulum-like oscillation is finally obtained through calculation:

$$\begin{bmatrix}\dot{X}_x \\ \dot{X}_y\end{bmatrix}=\begin{bmatrix}A_x & 0 \\ 0 & A_y\end{bmatrix}\begin{bmatrix}X_x \\ X_y\end{bmatrix}+\begin{bmatrix}B_x & 0 \\ 0 & B_y\end{bmatrix}\begin{bmatrix}u_x \\ u_y\end{bmatrix} \tag{8}$$

where the state vector $X_x=[x,\alpha_x,\dot{x},\dot{\alpha}_x]^T, X_y=[y,\alpha_y,\dot{x},\dot{\alpha}_y]^T$, and

$$B_x=\begin{bmatrix}0\\0\\1\\-\frac{3}{4d}\end{bmatrix}, B_y=\begin{bmatrix}0\\0\\1\\-\frac{3}{4d}\end{bmatrix},$$

$$A_x=\begin{bmatrix}0 & 0 & 1 & 0\\ 0 & 0 & 0 & 1\\ 0 & 0 & 0 & 0\\ 0 & -\frac{3g}{4d} & 0 & 0\end{bmatrix},$$

$$A_y=\begin{bmatrix}0 & 0 & 1 & 0\\ 0 & 0 & 0 & 1\\ 0 & 0 & 0 & 0\\ 0 & -\frac{3g}{4d} & 0 & 0\end{bmatrix}$$

Table 1 gives the main parameters of the UAV system structure in this work.

III. Control Law Based on LFPIO

A. Features of pendulum-like oscillation.

As shown in the linear model, two four-order pendulum subsystems are independent from each other. Matrix A_x and A_y is similar to each other, so we can choose either of the two subsystems to analyze features of the UAV pendulum-like oscillation. The state space equation of the linearized X-subsystem is described as follows [16]:

$$\begin{cases}\dot{X}=EX+FU \\ Y=GX\end{cases} \tag{9}$$

where $X=[x_1,x_2,x_3,x_4]^T=[x,\beta_x,\dot{x},\dot{\beta}_x]^T$

$$E=\begin{bmatrix}0 & 0 & 1 & 0\\ 0 & 0 & 0 & 1\\ 0 & 0 & -0.6500 & 0.6500\\ 0 & -8.547 & 0.5669 & -0.3924\end{bmatrix}$$

$$F=\begin{bmatrix}0\\0\\1\\-0.872\end{bmatrix}, G=\begin{bmatrix}1 & 0 & 0 & 0\\ 0 & 1 & 0 & 0\\ 0 & 0 & 1 & 0\\ 0 & 0 & 0 & 1\end{bmatrix}$$

In the actual flight, assume there is an external disturbances such as winds which may cause damage, so the pendulum system gets an original state $\phi_x(0)=0,05rad$.

B. Control law design based on LQR

The inherent features of the UAV pendulum-like oscillation system and the responses shows in Fig.2. A mixed LQR controller based on LFPIO is developed in this section. The given quadratic performance index (10) obtains the minimum value. It is testified that the performance index (10) can reach its minimum by the designed linear control law in formula (11).

$$J=\int_0^\infty (X^TQX+u^TRu)dt \tag{10}$$

$$u(t)=-KX(t)=R^{-1}F^TPX(t) \tag{11}$$

The best matrix P can be calculated as follows:

$$E^TP+PE-PER^{-1}F^TP+Q=0 \tag{12}$$

Matrix Q and R can be defined in the form of $Q=diag(q_{11},q_{12},0,0), R=1$.

Input u is the control force on the suspension center. The corresponding pendulum-holding back control law from the LQR is descried as follows.

$$u=-KX=(-k_1x_1+k_2x_2+k_3x_3+k_4x_4) \tag{13}$$

where K represents the feedback parameters obtained for the LQR. X represents the states of the system, i.e. the angle of the pendulum, the position of the suspension center, the angular velocity of the pendulum and the speed of the suspension center.

The LFPIO based LQR controller for prohibiting UAV pendulum-like oscillation of the hover and stare state in presence of external disturbances can be illustrated with Fig.2.

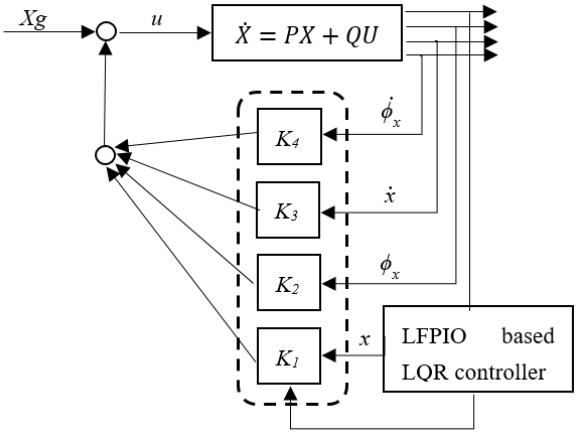

Fig.2 Structure of pendulum-like oscillation control system

C. Parameter optimization based on LFPIO

1） The Principle of PIO

Massive iron particles on the top of pigeon's beak has been found, which points to the north just as artificial compass, which help pigeons to determine their way home. Guilford and his colleagues state that homing pigeons may use different navigation tools in different parts of the journey. Pigeons may be more dependent on compass-like tools as they start their journey. Whilst they switch to using landmarks tools when they need to reassess their route in the latter part of their journey. The homing pigeon has an inborn homing ability to find its way home over extremely long distances by using three homing tools: magnetic field, sun and landmarks. Inspired by the above behaviors of pigeons, a new type of algorithm which is named pigeon-inspired optimization (PIO) has been invented by Duan in 2014 [14]. PIO is one of the newly bio-inspired algorithm proposed in the past few years for solving the complex optimization problems.

In order to avoid trapping into a locally optimal solution and find the optimal value correctly when solving multimodal problems. There are two operators using some rules to idealize the pigeons.

The first one is Map and Compass Operator. PIO update the current position of each particle in swarm by use the velocity vector. The velocity and position of pigeon i can be defined as V_i and X_i. The scheme for updating the velocity and position vector in iteration t is shown as follows:

$$V_i^t=V_i^{t-1}+rand^*(X_*-X_i^{t-1}) \tag{14}$$

$$X_i^t=X_i^{t-1}{}^*(1-e^{-R^*t})+V_i^t \tag{15}$$

where R denotes the map and compass factor and X_* is the current global best position that is located after comparing all the positions among all the pigeons.

The second one is landmark operator. Pigeons will fly straight to the place they want to go if they are familiar to the landmarks. They will follow the pigeons who are familiar to the landmarks whenever they are far from the destination and unfamiliar to the landmarks. Then half of the number of pigeons is decreased. We can find the center pigeon whose position is *Xc* from the left pigeons, the new position of others can be calculated by formula (16).

$$X_i(t+1)=X_i(t)+rand((X_c(t)-X_i(t)) \tag{16}$$

(1) Fitness function f

Fitness function f chosen in LQR controller and it can be shown as follows:

$$f=\frac{1}{\int_0^\infty (X^TQX+u^TRu)\ dt} \tag{17}$$

where $u=-(k_1x_1+k_2x_2+k_3x_3+k_4x_4)$,

$$K=[k_1,k_2,k_3,k_4]=lqr(A,B,Q,R),Q=diag(q_{11},q_{22},0,0)$$

(2) Population size Np, the map and compass factor R, the number of iteration t_1 and t_2, dimension D

According to the scale of the exact optimization problem, t_1 is considered the iterations of the map and compass operator, and t_2 will be the total iterations of the whole algorithm.

Here we choose Np=10. R=0.3. t_1 =60, t_2=40, D=2

2）Lévy-flight PIO

LFPIO is an algorithm evolved standard PIO algorithm by renew two operators instead of the old ones. Two new operators are given in this algorithm. A representative experiment confirms that the *Lévy-flight* PIO algorithm has a better performance than the PSO algorithm, SAPSO algorithm and PIO algorithm.

(a)Lévy-flight-based search operator

Lévy-flight is a Markov process as one of the best random walk models [17]. In the process of Lévy-flight's walk, the step length is a heavy-tailed distribution. The simplified Lévy-flight are shown as follows:

$$L(t)\sim|t|^{-1-\sigma},0<\sigma\leq2 \tag{18}$$

where t represents random step length. Because of the Lévy-flight's variance increases more rapidly, Lévy-flight is more effective than Brown motion when searching an unknown and large-scale space, the two kinds of variances are denoted as follows:

$$\begin{aligned}&\sigma^2(t)\sim t && \text{Brown motion}\\ &\sigma^2(t)\sim t^{3-\sigma},1<\sigma\leq2 && \text{Lévy-flight}\end{aligned} \tag{19}$$

In order to balance the diversity and the convergence speed in Lévy-flight, some solutions execute local search while others execute global search. In the meantime. Therefore, we use this mechanism to design the new search operator. By using Mantegna's algorithm, the operator of Lévy-flight can be implemented by following equations:

$$\begin{aligned}&s=\frac{\mu}{|v|^{\frac{1}{\delta}}},\delta=1.5\\ &\mu\sim N(0,\sigma_\mu^2),v\sim(0,\sigma_v^2)\\ &\sigma_\mu=\left\{\frac{\Gamma(1+\delta)sin(\frac{\pi\delta}{2})}{\Gamma[\frac{(1+\delta)}{2}]\delta\cdot2^{(\delta-1)/2}}\right\}^{1/\delta},\sigma_v=1\\ &step=s\circ(X_p(I-1)-X_{leader})\end{aligned} \tag{20}$$

$$X_t=X_p(I\text{-}1)+step\circ\boldsymbol{randn} \tag{21}$$

where N represents the normal distribution, s, step and X are vectors, $\circ$ is the Hadamard product, and ***randn*** is also a vector in which each element is a random number obeyed normal distribution. In addition, the elite selection strategy is utilized to improve the ability of local search and described by the following equation:

$$\begin{cases} X_p(I)=X_t, & if f_{cost}(X_t)<f_{cost}(X_p(I\text{-}1)) \\ X_p(I)=X_p(I\text{-}1), & if f_{cost}(X_t)\geq f_{cost}(X_p(I\text{-}1)) \end{cases} \tag{22}$$

(b) Improved landmark operator

The landmark operator can accelerate the convergence of algorithm In the PIO algorithm. Nevertheless, sometimes the operator might lead to the premature convergence, and the solution will be trapped into local minimum value. We adjust the step length of search to avoid this problem by adopt the adaptive logsig function:

$$\begin{aligned} X_t^i&=X_p^i(I\text{-}1)+Length\circ\boldsymbol{randn}\circ(X_{leader}\text{-}X_p^i(I\text{-}1)) \\ Length&=logsig(\tfrac{Nc\zeta\text{-}I}{k}) \end{aligned} \tag{23}$$

where i denotes the i-th dimension of solution, k and ζ are the adaptive parameters of logsig function. The parameter ζ decides by the time when the search converges. (k = 2.5, Nc = 100).

Algorithm 1 Lévy -flight -pigeon-inspired optimization
Input:
n : Population quantity in swarm
D: Dimension
Search range: the borders of the search space
R : The factor of map & compass
Nc_{max}: the max number of iterations
Np: numbers of pigeons
Output:
globalmin: The global minimum of the fitness function f
1 Initialization:
Set initial values for Nc_{max}, n , D, R, search range
,$X\,i$ and $V\,i$ for each individual
Set *globalmin* = $X\,i$, i =1
Calculate fitness values of different pigeon individuals
globalmin : arg min[$f(Xi)$]
2 Lévy-flights by Mantegna's algorithm
for n=1 to Nc_{max} **do**
  for i:=1 to Np **do**
    while $X\,i$ is beyond the search range **do**
      calculate Xc according to Eqs. (21) to (22)
    end while
  end for
evaluate Xc , and update *globalmin*
/* Xc : average value of the remaining individuals*/
calculate *step* according to Eq. (21)
for i:=1 to Np **do**
  evaluate $X\,g$,
end for
  update globalmin.
end for
3 results record
globalmin
f
End

Ⅳ. Experimental Results

In order to investigate the effectiveness and feasibility of the proposed LFPIO, we considered an external disturbances, we gives rise to pendulum oscillation without an appropriate control, the system gets an initial state x= [0, 0.05, 0, 0].

Using the proposed controller described in Fig.2 and experimental settings given in Section 3, the control parameters which include the optimal weight matrix Q and the resulting feedback vector K shows in Table Ⅱ.

Furthermore, we used a traditional method PSO, SAPSO and PIO instead of LFPIO as comparing experiments, all else being equal, as a compared experiment.

Fig.3 shows the evolution curve of algorithm for optimizing the weight parameters of the designed LQR controller. For the PSO, we set that c_1=1.3, c_2=1.8, D=2, N_p=10, Nc_{max}=100. For the SAPSO, we set that c_1=1.3, c_2=2.8, D=2,N_p=10, Nc_{max} =100. For the PIO and LFPIO, we set that solution space dimension D is 2, the population size Np=10, the map and compass factor R=0.2, and the number of iteration Nc_{max} =100.

Fig.3 shows the comparative evolutionary curves of the function. It can be seen from the figure that LFPIO achieves a better result with a lowest fitness value after 20 iterations of optimization, though it possess similar initial value. It is clear that both the time of convergence speed and the stabilized state in the experiment using LFPIO is better than the experiment using PSO, SAPSO and PIO.

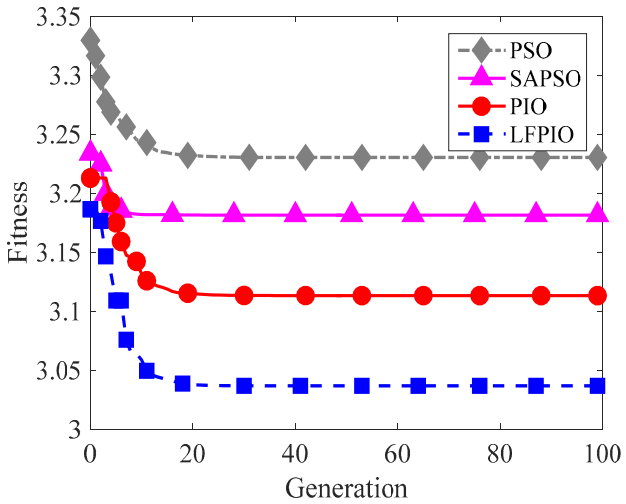

Fig.3 The average evolution curves of the PIO, LFPIO, PSO and SAPSO

V. Conclusions

A new LFPIO algorithm optimized approach pendulum-like oscillation controller in UAVs is described. The algorithm takes advantage of the accuracy and optimality of LQR. Compared with PSO, SAPSO and PIO, the experimental results show that the general optimized method, LFPIO, is better on accuracy, convergence speed and reliability. It seems to be more effective on helping the controller to meet greater precision. As a consequence, LFPIO can avoid the premature convergence problems and find the optimal value correctly. For future research, we can use our method in some other situations to find optimum solution and meet a better result.

Acknowlegment

This work was partially supported by National Natural Science Foundation of China under grant #61333004, and Aeronautical Foundation of China under grant #2015ZA51013

References

[1] Johnson E N and Turbe M A, "Modeling, control, and flight testing of a small-ducted fan aircraft," Journal of Guidance Control and Dynamics, vol.29, no.4, 2006, pp.769-779.

[2] Bloss R. "Latest unmanned vehicle show features both innovative new vehicles and miniaturization," Industrial Robot, vol.36, no.1, 2009, pp.13-18.

[3] Maravall D, Lope J D and Fuentes J P. "Vision-based anticipatory controller for the autonomous navigation of an UAV using artificial neural networks," Neurocomputing, vol.151, 2015, pp.101-107.

[4] Zhang J, Wu Y, Liu W and Chen X. "Novel approach to position and orientation estimation in vision-based UAV navigation," IEEE Transactions on Aerospace and Electronic Systems, vol.46, no.2, 2010, pp.687-700.

[5] Duan H B, S Shao, Su BW and Zhang L. "New development thoughts on the bio-inspired intelligence based control for unmanned combat aerial vehicle," Science China Technological Sciences, vol.53, no.8, 2010, pp.2025-2031.

[6] Li P and Duan H B, "Path planning of unmanned aerial vehicle based on improved gravitational search algorithm," Science China Technological Sciences, vol.55, no.10, 2012, pp.2712-2719.

[7] Duan H B, Zhang XY, Wu J and Ma GJ, "Max-min adaptive ant colony optimization approach to multi-UAVs coordinated trajectory re-planning in dynamic and uncertain environments," Journal of Bionic Engineering, vol.6, no.2, June 2009, pp.161-173.

[8] Rakotomamonjy T, Ouladsine M and Moing T L. "Longitudinal modelling and control of a flapping-wing micro aerial vehicle," Control Engineering Practice, vol.18, no.7, 2010, pp.679-690.

[9] Duan H B, Sun C H. "Pendulum-like oscillation controller for micro aerial vehicle with ducted fan based on LQR and PSO". Science China Technological Sciences, vol.56, no.2, 2013, pp423-429.

[10] Dufrene W R. "Application of artificial intelligence techniques in uninhabited aerial vehicle flight," Proceedings of the 22nd Digital Avionics Systems Conference, 2003.

[11] Yu Y C, Duan H B. "A quantum-behaved particle swarm optimization approach to PID control parameters tuning" Proceedings of the 32nd Chinese Control Conference, 26-28 July 2013, Xi'an, pp.7949-7954

[12] Kenndy J, Eberhart R C. "Particle swarm optimization," in proceedings of the 1995 IEEE International Conference on Networks, Perth, Australia, 1995, pp.1942-1948

[13] Shieh H L, Kuo C C, Chiang C M. "Modified particle swarm optimization algorithm with simulated annealing behavior and its numerical verification." Applied Mathematics & Computation, vol.218, no.8, 2011, pp.4365-4383.

[14] Duan H B and Qiao P X. "Pigeon-inspired optimization: A new swarm intelligence optimizer for air robot path planning," International Journal of Intelligent Computing and Cybernetics, vol.7, no.1, 2014, pp.24-37.

[15] Pflimlin J M, Binetti P, Soueres P, Hamel T and Trouchel D. "Modeling and attitude control analysis of a ducted-fan micro aerial vehicle," Control Engineering Practice, vol.18, no.3, 2010, pp.209–218.

[16] Sun C H and Duan H B. "Artificial Bee Colony Optimized Controller for MAV Pendulum," Aircraft Engineering and Aerospace Technology, vol.85, no.2, 2013, pp.104-114.

[17] Sheng Z. "Parameter estimation of atmospheric refractivity from radar clutter using the particle swarm optimization via Lévy flight," Journal of Applied Remote Sensing, vol.9, no.1, 2015, pp.378–387.

Appendix

TABLE I. Main parameters of the UAV system structure

Symbol	Value	Physical meaning
g	$9.8m/s^2$	gravity acceleration
d	$0.86m$	pendulum length
m_t	20kg	pendulum quality
m	10kg	suspension center
β_x, β_y	—	pitch and roll angle
α_x, α_y	—	pendulum angle
u_x, u_y	—	control force on O_h

TABLE II. Control parameters of the LFPIO based LQR approach

Parameter	Optimized value
Matrix Q	Diag(245.6,250.3 0,0)
Feedback vector K	[9.9598 -17.2437 6.7924 0.9811]